PNAS RESEARCH ARTICLE | BIOCHEMISTRY

Neuronal differentiation requires BRAT1 complex to remove REST from chromatin

Sadat Dokaneheifard[a], Helena Gomes Dos Santos[a], Monica Guiselle Valencia[a], Harikumar Arigela[a], Raghu Ram Edupuganti[a], and Ramin Shiekhattar[a,1]

Edited by Shelley Berger, University of Pennsylvania, Philadelphia, PA; received October 26, 2023; accepted April 17, 2024

Repressor element-1 silencing transcription factor (REST) is required for the formation of mature neurons. REST dysregulation underlies a key mechanism of neurodegeneration associated with neurological disorders. However, the mechanisms leading to alterations of REST-mediated silencing of key neurogenesis genes are not known. Here, we show that BRCA1 Associated ATM Activator 1 (BRAT1), a gene linked to neurodegenerative diseases, is required for the activation of REST-responsive genes during neuronal differentiation. We find that INTS11 and INTS9 subunits of Integrator complex interact with BRAT1 as a distinct trimeric complex to activate critical neuronal genes during differentiation. *BRAT1* depletion results in persistence of REST residence on critical neuronal genes disrupting the differentiation of NT2 cells into astrocytes and neuronal cells. We identified BRAT1 and INTS11 co-occupying the promoter region of these genes and pinpoint a role for BRAT1 in recruiting INTS11 to their promoters. Disease-causing mutations in *BRAT1* diminish its association with INTS11/INTS9, linking the manifestation of disease phenotypes with a defect in transcriptional activation of key neuronal genes by BRAT1/INTS11/INTS9 complex. Finally, loss of *Brat1* in mouse embryonic stem cells leads to a defect in neuronal differentiation assay. Importantly, while reconstitution with wild-type BRAT1 restores neuronal differentiation, the addition of a BRAT1 mutant is unable to associate with INTS11/INTS9 and fails to rescue the neuronal phenotype. Taken together, our study highlights the importance of BRAT1 association with INTS11 and INTS9 in the development of the nervous system.

BRAT1 | Integrator | REST | neuronal differentiation | transcription

Significance

Neurodegenerative diseases affect millions of people worldwide. Such diseases occur following the loss of nerve cells in the brain or peripheral nervous system. While the identity of a number of genes whose mutations result in neuronal loss is known, their functional connection to neurodegeneration remains to be elucidated. In this study, we show *BRAT1*, a gene linked to neurodegenerative diseases in children, regulates the occupancy of critical neuronal silencer Repressor element-1 silencing transcription factor (REST) during neuronal differentiation. The absence of BRAT1 leads to deregulation of REST-responsive genes and loss of neuronal differentiation.

BRAT1 (BRCA1 Associated ATM Activator 1), also known as *BAAT1* (BRCA1-associated protein required for ATM activation 1), was initially described as a BRCA1-interaction partner and was deemed important for activation of ATM (1). It was reported that BRAT1 protein localizes to both nucleus and cytoplasm (2). Later studies suggested the involvement of BRAT1 in DNA damage response as well as mTOR signaling (1, 3–6). *Brat1* depletion resulted in impaired cell cycle progression using synchronized mouse embryonic fibroblasts (MEF) under serum-starvation condition (5). Upregulation of serum anti-BRAT1 antibodies was indicated as a common molecular biomarker for gastrointestinal cancers and atherosclerosis (7). Although BRAT1 has been deemed undruggable, recently the small molecule, Curcusone D, was shown to associate with BRAT1 and reduce cancer cell migration (8). *Brat1* was found to be highly expressed in mouse brain (4). Consistent with functional importance of BRAT1 in the brain, germ line mutations in *BRAT1* are associated with rigidity and multifocal seizure syndrome, lethal neonatal, and neurodevelopmental disorder with cerebellar atrophy and with or without seizure (9–14). BRAT1-related genes are broadly found in eukaryotes (source: eggnog v.6, ID: 5EM9B, 441 evolutionary related proteins) (15). While the protein domain composition is weakly conserved [source: Pfam (16)], BRAT1 orthologs have a common theme of Leucine-rich repeats folding into helical structures [source: CATH classification 1.25.10.10 (17)]. Human BRAT1 has been described to contain a CIDE-N [cell death–inducing DFF45-like effector (CIDE) domain] at its N terminus and two HEAT (Huntingtin, Elongation factor 3, A subunit of protein phosphatase 2A, and TOR1; aa 495-531, aa 544-576) repeats at its C terminus (4).

Repressor element-1 (RE1) silencing transcription factor (REST), also known as neuron-restrictive silencer factor (NRSF) is a zinc finger transcription factor widely expressed in embryogenesis required for repressing neuronal gene transcription in non-neuronal cells by binding to the consensus RE1 site (18–20). REST silences the expression of a wide range of target genes involved in neuron-specific functions such as synaptic vesicle proteins and neurotransmitter receptors (19). REST dysregulation is involved in neurodegenerative diseases in human and is thought to underly a key mechanism of

Author affiliations: [a]Department of Human Genetics, University of Miami, Miller School of Medicine, Sylvester Comprehensive Cancer Center, Miami, FL 33136

Author contributions: S.D., H.A., H.G.D.S., and R.S. designed research; S.D., M.G.V., and R.R.E. performed research; S.D. contributed new reagents/analytic tools; S.D., M.G.V., and H.G.D.S. analyzed data; and S.D., H.G.D.S., and R.S. wrote the paper.

The authors declare no competing interest.

This article is a PNAS Direct Submission.

[1]To whom correspondence may be addressed. Email: rshiekhattar@med.miami.edu.

This article contains supporting information online at https://www.pnas.org/lookup/suppl/doi:10.1073/pnas.2318740121/-/DCSupplemental.

Published May 28, 2024.

progressive neurodegeneration associated with neurological disorders (18, 20, 21). However, the mechanisms leading to alterations of REST-mediated silencing of key neurogenesis genes are not known.

Integrator is an evolutionarily conserved complex in metazoans containing at least 16 subunits (22–25) associated with the C-terminal domain (CTD) of RNA polymerase II (RNAPII) (22, 24–27). Since its discovery, Integrator has been shown to be implicated in multiple pathways involving coding and noncoding RNA processing and transcriptional regulation (28). Recent studies have highlighted a role for Integrator in transcriptional initiation, pause release, elongation, as well as termination of protein-coding genes (29–31). Additionally, Integrator was shown to be involved in biogenesis of enhancer RNAs (eRNAs) (32) and transcriptional responsiveness to epidermal growth factor (EGF) signaling (32). Integrator was shown to play diverse roles in ciliogenesis (33), embryogenesis (34), human lung function (35), adipose differentiation (36), and maturation of viral microRNAs (37, 38). We recently pinpointed a function for Integrator in the maintenance of canonical mature microRNAs stability through facilitating the loading of AGO2 (39). Importantly, mutations in human Integrator complex have been linked to brain developmental syndrome and cerebellar atrophy (40, 41).

The key catalytic subunit of Integrator, INTS11, forms a heterodimer with INTS9 (42) mediated by the C-terminal regions of each protein module (27). INTS4, a HEAT repeat-containing protein, was determined to be a direct interaction partner of the INTS9/INTS11 heterodimer forming the minimal Integrator cleavage module (23). INTS4 was suggested to play a "Symplekin-like" scaffold making specific and conserved interaction with INTS9/INTS11 (26). We find that BRAT1 associates with INTS9/INTS11 heterodimer, and this complex does not contain INTS4 protein. Indeed, our molecular modeling suggests that BRAT1 folds into a helical "O" shape structure wrapping around the INTS9/INTS11 heterodimer which partially overlaps with the interface that binds INTS4. Therefore, we find BRAT1 and INTS4 form mutually exclusive complexes with INTS11/INTS9 heterodimer. Importantly, disease-causing mutations of BRAT1 display diminished interaction with INTS11/INTS9. We show that during neuronal differentiation of NT2 cells, BRAT1 occupies and activates the expression of REST-responsive genes critical for neurodevelopment. Indeed, in the absence of BRAT1, there is a persistence residence of REST and lack of activation of key genes involved in neurulation. Taken together, our study reveals an association of BRAT1 with INTS11/INTS9 proteins to regulate a set of key neuronal genes involved in differentiation of NT2 cells into a neuronal fate. We were able to demonstrate a similar role for BRAT1 during differentiation of embryonic mouse stem cells into neurons with key requirement of BRAT1 association with INTS11/INTS9 proteins.

Results

Integrator Subunits INTS9 and INTS11 Interact with BRAT1. We found integrator as a complex that associates with the C-terminal domain (CTD) of RNA polymerase II (RNAPII) (22, 28). To fully define the Integrator complex subunit composition, we isolated Flag-INTS11 from HEK293T-derived stable cell line and subjected the affinity-purified fractions to mass spectrometry. Beyond the core components of integrator complex described previously (22), we obtained sequences corresponding to BRAT1 protein (Fig. 1*A* and Dataset S1). Western blot analysis of affinity-purified fractions confirmed the specific association of BRAT1 with components of Integrator complex isolated through affinity purification of INTS11 (Fig. 1*B*). We next developed a HEK293T-derived cell line stably expressing Flag-BRAT1 to rigorously define the composition of the BRAT1-containing complex(s) (Fig. 1*C*). Affinity purification of Flag-BRAT1 followed by western blot analyses and silver staining (Fig. 1*C*) identified the core catalytic subunits of Integrator complex, INTS11 and INTS9, as the key components of the BRAT1-containing complex. Beyond INTS11 and INTS9, we did not find any other subunits of Integrator complex in association with BRAT1 (Fig. 1*C*). To define the molecular mass of the BRAT1/INTS11/INTS9 complex, we subjected the affinity-purified BRAT1 preparation to Superose 6 gel filtration chromatography (Fig. 1*D*) followed by mass spectrometry (Fig. 1*D* and Dataset S2). BRAT1 protein eluted with INTS11 and INTS9 at fraction 34 which was confirmed by western blot analyses, silver staining, and mass spectrometry (Fig. 1*D* and Dataset S2).

BRAT1 Interacts with INTS11/INTS9 in NT2 Cells, and It Is Required for the Differentiation of the NT2 Cells into Neurons and Astrocytes. NTERA-2 (also known as NT2) cells are clonally derived human embryonal carcinoma cell line that can be differentiated into a neuronal lineage following exposure to all-trans retinoic acid (ATRA) (43, 44). Since BRAT1 is associated with neurodevelopmental disorders (9–14), we sought to determine the interaction between BRAT1 and INTS11/NTS9 in NT2 cells. We performed endogenous immunoprecipitation (IP) followed by western blot analysis (Fig. 2*A*) in NT2 cells. BRAT1 antibody immunoprecipitated INTS11 and INTS9 confirming our results from HEK293T cells. Additionally, immunoprecipitated eluate using INTS11 and INTS9 antibodies contained not only BRAT1 but also INTS4, reflecting the association of INTS11/INTS9 with two distinct complexes of Integrator and a second smaller complex containing BRAT1 (Fig. 2*A*).

NT2 cells exposed to ATRA for 14 d develop into a preneuronal disc-like foci (Fig. 2*B*). A more prolonged (28 d) exposure of NT2 cells to ATRA results in the appearance of neuronal and glial phenotypes (Fig. 2*B*). To assess the role of BRAT1 in neurogenesis, we depleted BRAT1 using an inducible short hairpin RNA (shRNA) in NT2 cells while treating the cells with ATRA to determine their differentiation into a neuronal and a glial cell fate (Fig. 2*B*). Importantly, depletion of BRAT1 in NT2 cells did not result in any changes in their growth rate (*SI Appendix*, Fig. S1*A*) and the protein level of Integrator subunits as measured by western blot analyses (Fig. 2*C* and *SI Appendix*, Fig. S1*B*). Notably, we detected an increase in a TUBB3, a neural marker (43, 45, 46), and GFAP, an astrocyte (glial) marker (43, 47), following 28 d of ATRA treatment (Fig. 2*C*, lane 2). Additionally, we observed a reduction in OCT4 and SOX2, as the key stem cell factors, reflective of a loss of stemness and a gain of neuronal and glial phenotypes (Fig. 2*C*, lane 2). Critically, depletion of BRAT1 during the differentiation protocol led to a decreased expression of both TUBB3 and GFAP (Fig. 2*C*, lane 3). Consistent with the loss of TUBB3 and GFAP, depletion of BRAT1 decreased preneuronal foci formation following 14 d of ATRA treatment (Fig. 2 *D* and *E*). Indeed, depletion of BRAT1 abrogated the establishment of neuronal and astrocyte phenotypes as measured by TUBB3, GFAP, or MAP2 (43, 46) expression by day 28 or the late neuronal marker, Synapsin1 (43), after 42 d of ATRA treatment (Fig. 2 *F*–*H*). Taken together, these results point to a role for BRAT1 in neuronal and astrocytes differentiation in human NT2 cells.

BRAT1 Depletion Leads to a Defect in the Expression of Critical Genes for Neuronal Function. To determine *BRAT1*-mediated changes in gene expression during the ATRA-induced differentiation of NT2 cells, we depleted *BRAT1* and analyzed the transcriptome of NT2 cells. ATRA treatment in the control cells resulted in the differential expression of 11,570 genes following 28 d where 5,687 genes (49%) were down-regulated and a similar number of 5,883 genes (51%) were up-regulated (1.5-fold change and false discovery

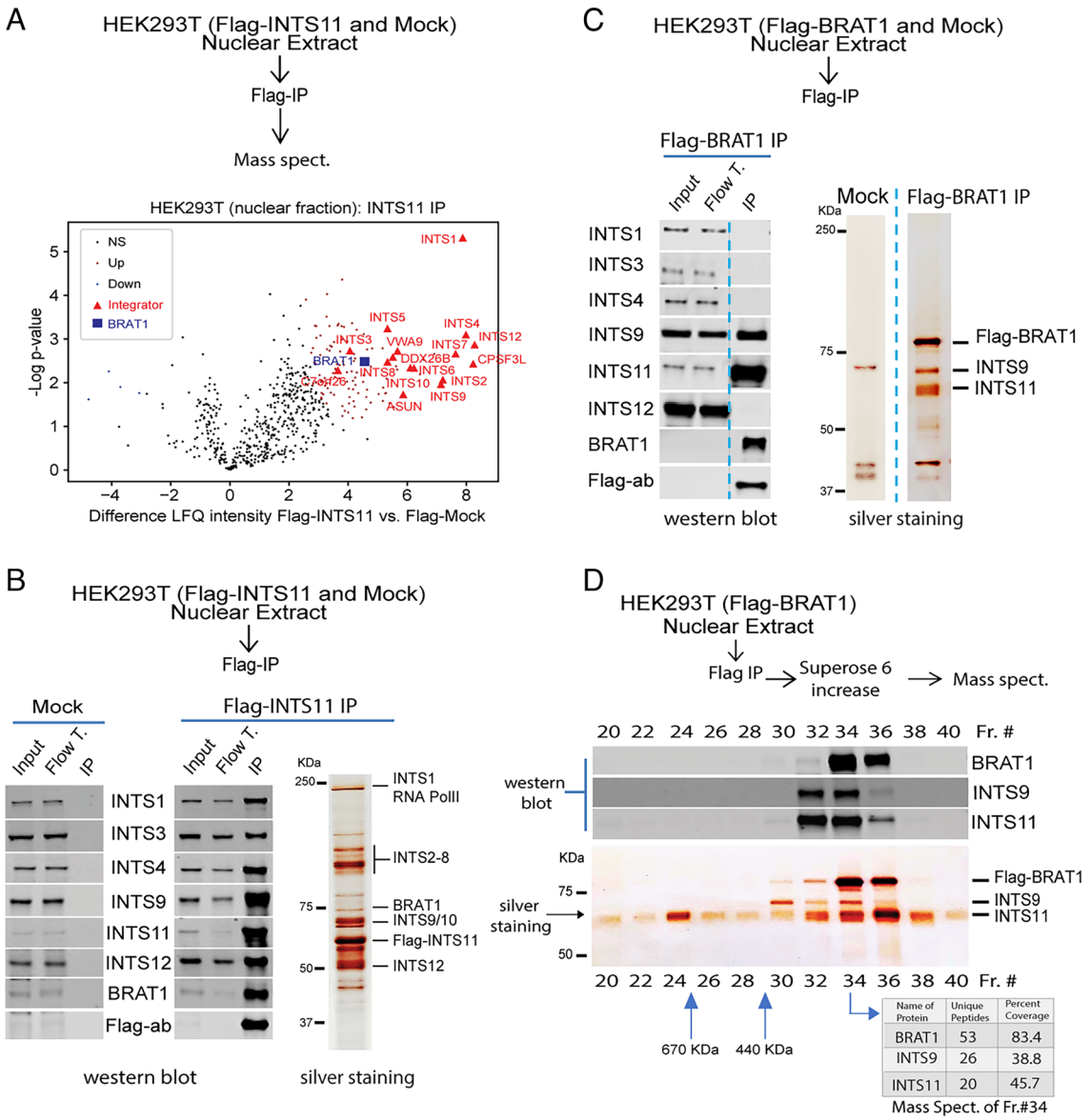

Fig. 1. BRAT1 forms a stable interaction with INTS9/INTS11 heterodimer. (*A*) Purification scheme and volcano plot of the protein enrichment in nuclear extract of HEK293T cells detected by mass spectrometric label-free quantification (LFQ) for Flag-INTS11 vs. mock (two replicates per condition). Enriched proteins are shown as red circles and depleted proteins as blue circles, no significant protein interactors are shown as black circles. The enrichment levels of the full Integrator complex (red triangles) and BRAT1 (blue square) are highlighted (gene nomenclature: CPSF3L = INTS11, ASUN = INTS13, VWA9 = INTS14). (*B*) Western blot of affinity-purified Flag-INTS11 and mock along with the silver staining of affinity-purified Flag-INTS11. (*C*) Western blot and silver staining of affinity-purified Flag-BRAT1 from nuclear lysate of HEK293T cells stably expressing Flag-BRAT1. Mock was used as control. (*D*) Affinity-purified Flag-BRAT1 from nuclear extract of HEK293T cells stably expressing Flag-BRAT1 was fractionated on Superose 6 increase gel filtration and then visualized by western blot (*Top* side) and silver staining (*Bottom* side). Fraction numbers are indicated on *Top* and *Bottom* of the blot. Mass spectrometry on fraction 34 of nuclear extract of HEK293T cells stably expressing Flag-BRAT1 fractionated on Superose 6 increase gel filtration is shown by the table. Result confirmed the coelution of BRAT1 with INTS11/INTS9 heterodimer in fraction 34. Number of unique peptides and their percent coverage for BRAT1/INTS11/INTS9 interactors are provided in the illustrated table.

rate FDR < 0.05) (*SI Appendix*, Fig. S2*A*). Next, we depleted *BRAT1* during the 28 d of differentiation and assessed the differential gene expression in NT2 cells undergoing neurogenesis. Remarkably, the loss of *BRAT1* culminated in the decreased expression of a relatively small set of genes (250) (Fig. 3 *A* and *B* and Dataset S3). Critically, the prominent number of down-regulated genes play key roles in neuronal function including synaptic transmission and axonal guidance (Fig. 3*C* and Dataset S4). In contrast, differentially up-regulated genes (126) (Fig. 3 *A* and *B* and Dataset S3) control extracellular matrix organization and proliferation functions distinct from neuronal phenotype (*SI Appendix*, Fig. S2*B*). These gene expression changes were validated using RT-qPCR (Fig. 3 *D*–*H*). Taken together, our data suggest that BRAT1 is important for the expression of the genes involved in neuronal functions.

BRAT1 Regulates INTS11 Residence at Critical Neuronal Differentiation Genes to Overcome REST-Mediated Repression. To determine the dynamic changes for BRAT1 and INTS11 proteins during the differentiation of NT2 cells into the neural lineage, we performed chromatin immunoprecipitation qPCR (ChIP-qPCR) following ATRA-mediated differentiation (Fig. 4*A*). While ChIP-qPCR indicated the occupancy of BRAT1 and INTS11 at the promoter region of neural genes prior to stimulation with ATRA, we found a significant increase in INTS11 and BRAT1 residence at genes induced by ATRA following the differentiation protocol (Fig. 4*A*). We next asked whether BRAT1 regulates the occupancy of INTS11 at the promoter of BRAT1-responsive genes. ChIP-qPCR was performed using specific antibodies against BRAT1 and INTS11 in NT2 cells 3 d after *BRAT1* depletion (Fig. 4*B*). Importantly, depletion of *BRAT1*

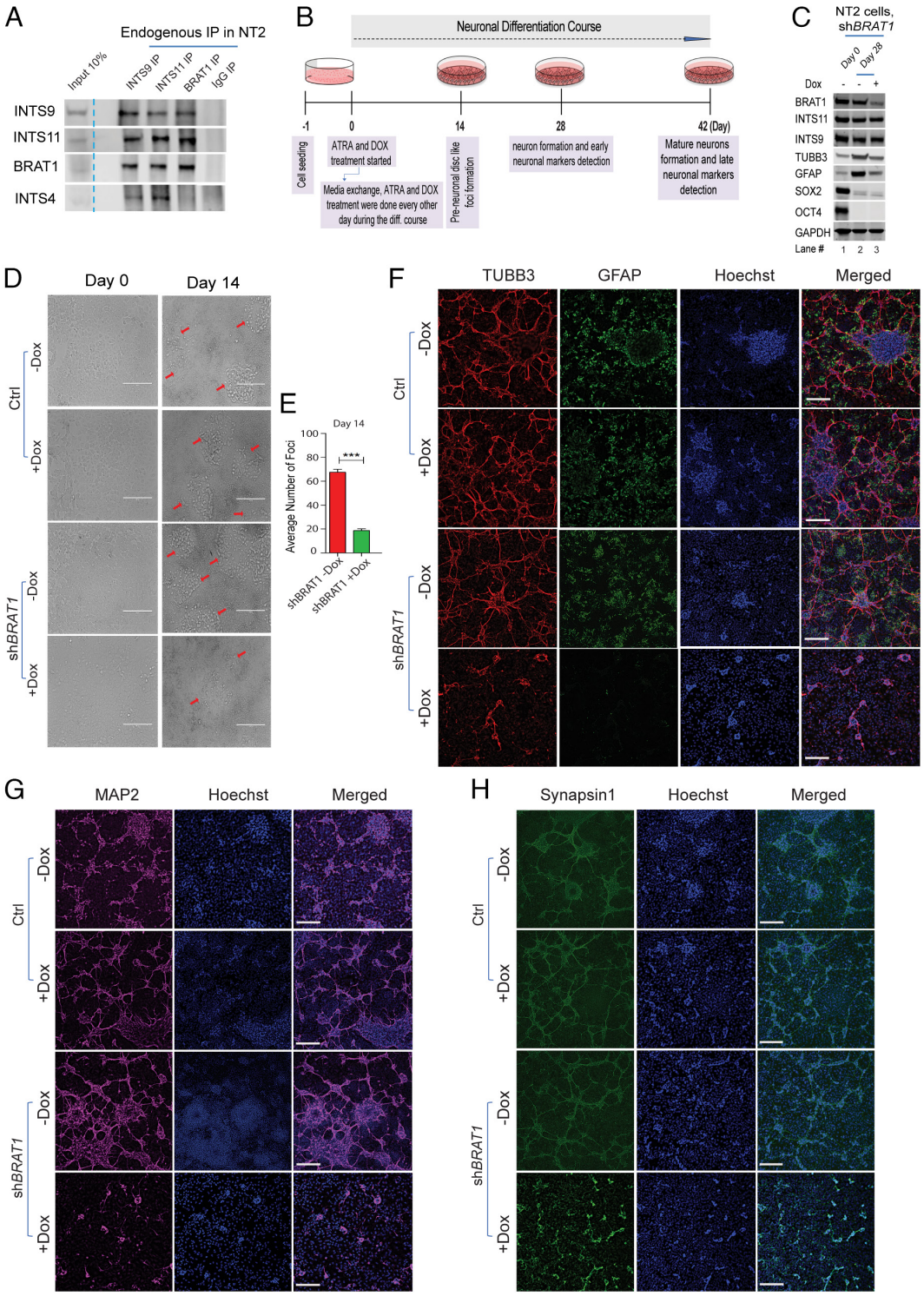

Fig. 2. BRAT1 associates with INTS9/INTS11 heterodimer in NT2 cells and it is required for differentiation of NT2 cells into neurons and astrocytes. (*A*) Immunoprecipitation of endogenous BRAT1, INTS11, and INTS9 in NT2 cells. The immunoblots of antibodies against INTS11 and INTS9 coimmunoprecipitated with BRAT1 and INTS4. Reciprocally, immunoblot antibody against BRAT1 coimmunoprecipitated only with INTS9 and INTS11. IgG was used as the negative control. Data show the presence of the trimeric BRAT1/INTS11/INTS9 complex in NT2 cells. (*B*) Diagram of the ATRA-treated based protocol used for the differentiation of NT2 cells. (*C*) Western blot of BRAT1, INTS9, and INTS11 in parallel with stemness, neuronal, and astrocyte markers 28 d postdifferentiation of NT2 cells in *BRAT1*-depleted cells compared to control cells. Data show that TUBB3 and GFAP protein levels decreased following *BRAT1* depletion (lane 3) compared to nondepleted *BRAT1* cells (lane 2) 28 d following ATRA treatment. (*D*) Cell plate images showing the changes in cluster formation (bright and disc-like structures, highlighted by the red arrows) of NT2 cells at 14 d postdifferentiation for *BRAT1*-depleted cells compared to control cells. Cells were imaged BF (bright field) with a EVOS XL Core Imaging System (Life Technologies) by a 20× objective. Final resolution figures were processed by ImageJ Fiji online tool (https://ij.imjoy.io/). (Scale bar: 200 μm.) (*E*) Bar plot of the average number of cell clusters (foci or bright and disc-like structures) per area at day 14, with Nikon TMS by a 4× objective. Data show that the average number of the clusters per area is significantly reduced in *BRAT1*-depleted cells compared to nondepleted cells 14 d post-differentiation (***$P < 0.001$). (*F*) Representative immunofluorescence images of TUBB3 (red, Biolegend #801201), GFAP (green, Invitrogen, #13-0300), Hoechst (blue), and merged images in NT2 cells 28 d postdifferentiation. (*G*) Representative immunofluorescence images of MAP2 (magenta, Millipore #AB5622), Hoechst (blue), and merged images in NT2 cells 28 d postdifferentiation. (*H*) Representative immunofluorescence images of Synapsin1 (green, Synaptic Systems #106 011C3), Hoechst (blue), and merged images in NT2 cells 42 d post-differentiation. The scale bar for the microscopy images in panels (*F–H*) is 200 μm.

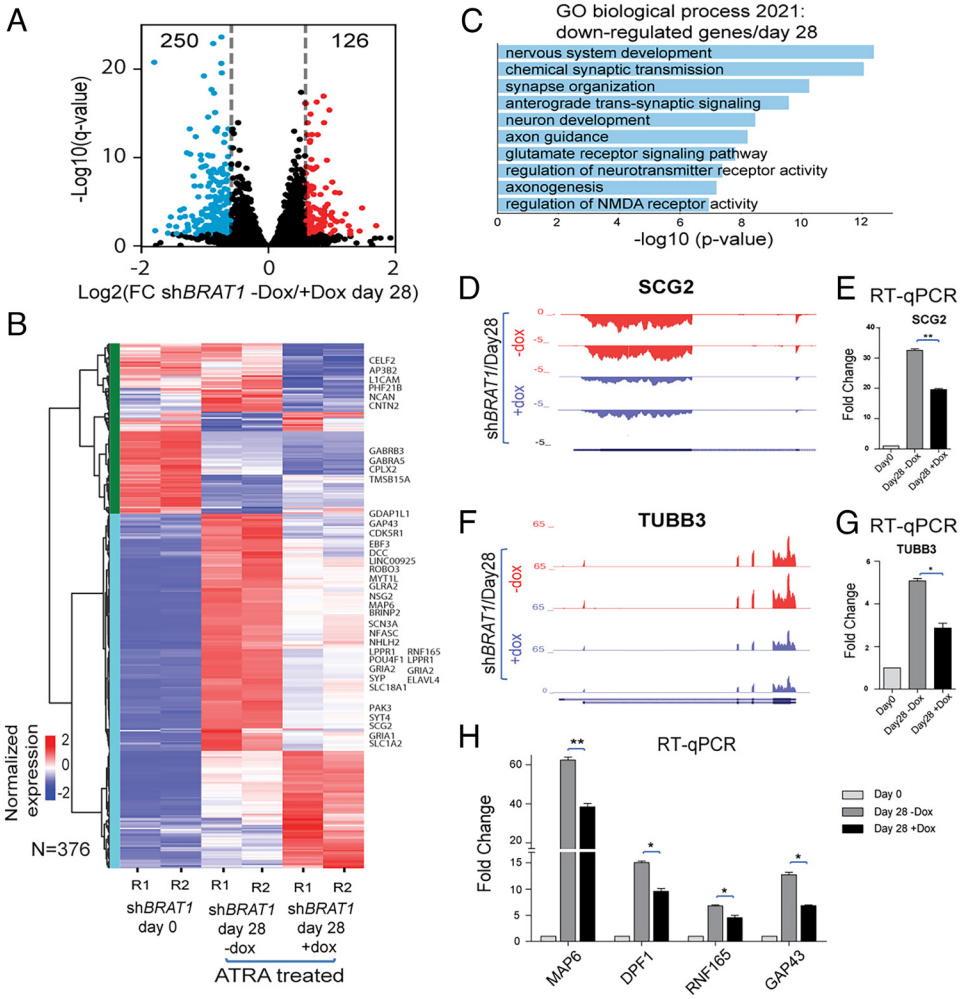

Fig. 3. BRAT1 mediates the expression of a critical neurodevelopmental genes. (*A*) Volcano plot of BRAT1-depleted cells compared to the cells expressing normal level of BRAT1 28 d post-ATRA treatment of NT2 cells, with down-regulated genes in blue, up-regulated genes in red and nonsignificant gene changes in black (significance cutoffs: 1.5-fold change and FDR < 0.05). (*B*) Heat map of the 376 genes differentially expressed from panel (*A*). showing the row normalized gene expression levels (z-score) in control and BRAT1-depleted cells at day 0 (pretreatment) and day 28 postdifferentiation with ATRA treatment. Left color bar represent the clusters obtained by unsupervised hierarchical clustering (method = ward, metric = Euclidean distance). Genes listed on the right side are involved in neural development. (*C*) Gene enrichment of the down-regulated genes against Gene Ontology (GO) biological process 28 d after *BRAT1* depletion in differentiated NT2 cells compared to the cells expressing normal level of BRAT1. Of the top 10 GO biological processes, most are categories associated with the nervous system including nervous system development, chemical synaptic transmission, and synapse organization. (*D*) Genome browser tracks of the normalized RNA-seq data at SCG2 gene locus [28-d post-ATRA treatment, control cells expressing normal level of BRAT1 in red (−Dox), and *BRAT1*-depleted cells in blue (+Dox), two replicates each]. (*E*) Bar plot of the fold change in SCG2 gene expression of each sample compared to control by RT-qPCR (two replicates). Expression was significantly decreased after *BRAT1* depletion (+Dox) compared to the cells expressing normal level of BRAT1 (−Dox) at day 28 of ATRA treatment. (*F*) Genome browser tracks of the normalized RNA-seq data for TUBB3 gene locus [28-d post-ATRA treatment, control cells expressing normal level of BRAT1 in red (−Dox), and *BRAT1*-depleted cells in blue (+Dox), two replicates each]. (*G*) Bar plot of the fold change in TUBB3 gene expression of each sample compared to control by RT-qPCR (two replicates). Expression was significantly decreased after *BRAT1* depletion (+Dox) compared to the cells expressing normal level of BRAT1 (−Dox) at day 28 of ATRA treatment. (*H*) RT-qPCR data for showing additional examples of neural marker genes whose expressions are decreased 28 d post-differentiation in *BRAT1*-depleted cells (+Dox) compared to cells expressing normal level of BRAT1 (−Dox). For RT-qPCR experiments, data are expressed as ±SEM (two repeats). Statistical significance was determined by unpaired *t* test (**P* < 0.05, ***P* < 0.01).

led to a significant reduction of INTS11 occupancy (Fig. 4*B*). Taken together, these results demonstrate that BRAT1 and INTS11 are concomitantly recruited during neural differentiation of NT2 cells to control the expression of the neural genes, and BRAT1 regulates the residence of INTS11 at the promoter of BRAT1-responsive genes.

Since ~88% of genes that are down-regulated following *BRAT1* depletion are the targets of the neuronal silencer REST (RE1 Silencing Transcription Factor) (Dataset S5) (18, 20), we asked whether during neuronal differentiation, BRAT1 functions to overcome REST-mediated repression. We measured REST residence prior and 28 d following neuronal differentiation in NT2 cells. Importantly, 28 d following neuronal differentiation REST no longer occupies key neuronal genes (Fig. 4*C*). However, loss of *BRAT1* leads to a persistent residence of REST at all neuronal genes examined (Fig. 4*C*). These results highlight the importance of BRAT1 during neuronal differentiation in overcoming REST-mediated repression and induction of differentiation.

Pathogenic E522K Mutation in BRAT1 Disrupts Its Interaction with INTS11/INTS9 Heterodimer. Recent reports link mutations in human Integrator subunits to neurodevelopmental syndromes and developmental ciliopathy (40, 41). Similarly, mutations in *BRAT1* have been associated with neurodevelopmental and neurodegenerative disorders manifested with varying degrees of clinical severity (9–14). These include rigidity and multifocal seizure syndrome, lethal neonatal rigidity, and epilepsy of infancy with migrating focal seizures (9–14). In order to further delineate the interaction between BRAT1 with INTS11/INTS9, we examined the effect of several patient-derived mutations of BRAT1 on its interaction with INTS11/INTS9 heterodimer (Fig. 5*A*). Human BRAT1 is a protein of 821 amino

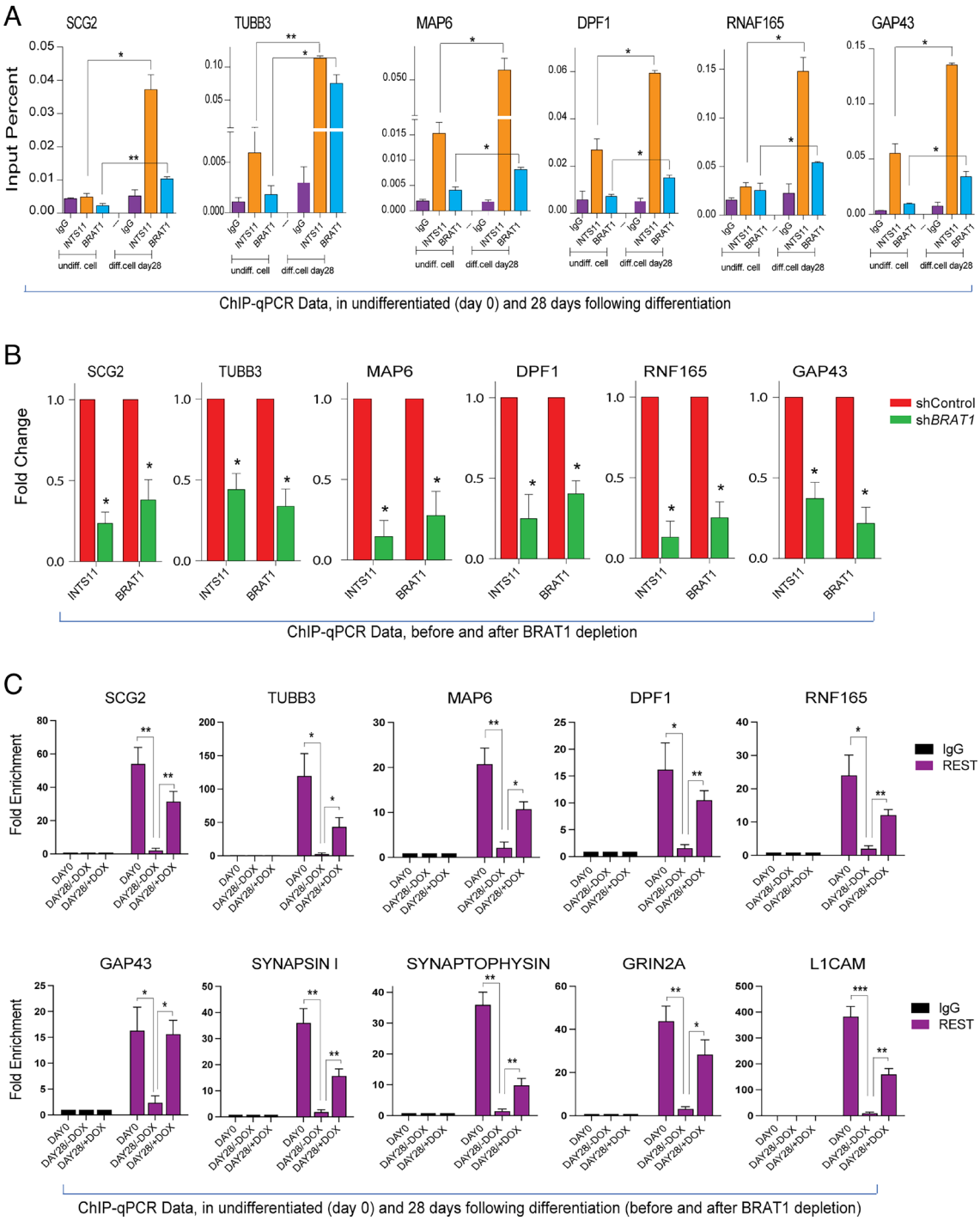

Fig. 4. BRAT1 and INTS11 co-occupy the promoter of neuronal genes and regulate the occupancy of REST. (*A*) Bar plots of INTS11 and BRAT1 ChIP-qPCR data at day 0 (undifferentiated cells) and at day 28 post-differentiation of NT2 cells showing significant increase of BRAT1 and INTS11 co-occupancy at the promoter region of neuronal genes activated following 28 d of ATRA treatment (normal differentiation). Each of data in the differentiated condition has been compared with its equivalent in the undifferentiated condition. (*B*) Bar plots of INTS11 and BRAT1 ChIP-qPCR data reveal the reduced enrichment of BRAT1 and INTS11 at the promoter region of neural marker genes following *BRAT1* depletion (3 d after adding Dox without ATRA treatment) in sh*BRAT1* NT2 cells compared to shControl cells. (*C*) Bar plots of REST ChIP-qPCR data at day 0 (undifferentiated cells) and 28 d following ATRA treatment (differentiated cells) of NT2 cells. Each data in REST IP condition is normalized to its equivalent IgG condition. For ChIP-qPCR, data are expressed as ±SEM fold change over shControl cells (two repeats). Statistical significance was determined by unpaired *t* test (*$P < 0.05$, **$P < 0.01$).

acids in length (protein id: NP_689956.2, gene id: NM_152743.4) displaying sequence conservation among vertebrates (Fig. 5*B*). We selected three of the reported neural disease-associated BRAT1 mutations including E522K (48), V62E (49), and del_P309-Q310 (50) and mapped these mutations on the predicted three-dimensional model for human BRAT1 (Fig. 5*C*). Additionally, using published structure for INTS11/INTS9 heterodimer, we derived the BRAT1/INTS11/INTS9 trimeric structure (Fig. 5*D*). In this model, we assume INTS11 and INTS9 interact with each other at their C-terminal regions as previously described (26, 27), while BRAT1 is predicted to fold as a circular helical structure around the stem of the structure holding INTS11/INTS9 heterodimer (Fig. 5*D*). This structural model suggests that BRAT1 and INTS4 interaction interfaces with INTS11/INTS9 heterodimer partially overlap and consequently form two mutually exclusive complexes of INTS11/INTS9/INTS4 or INTS11/INTS9/BRAT1 (Fig. 5*E* shows the multiple clashes between BRAT1

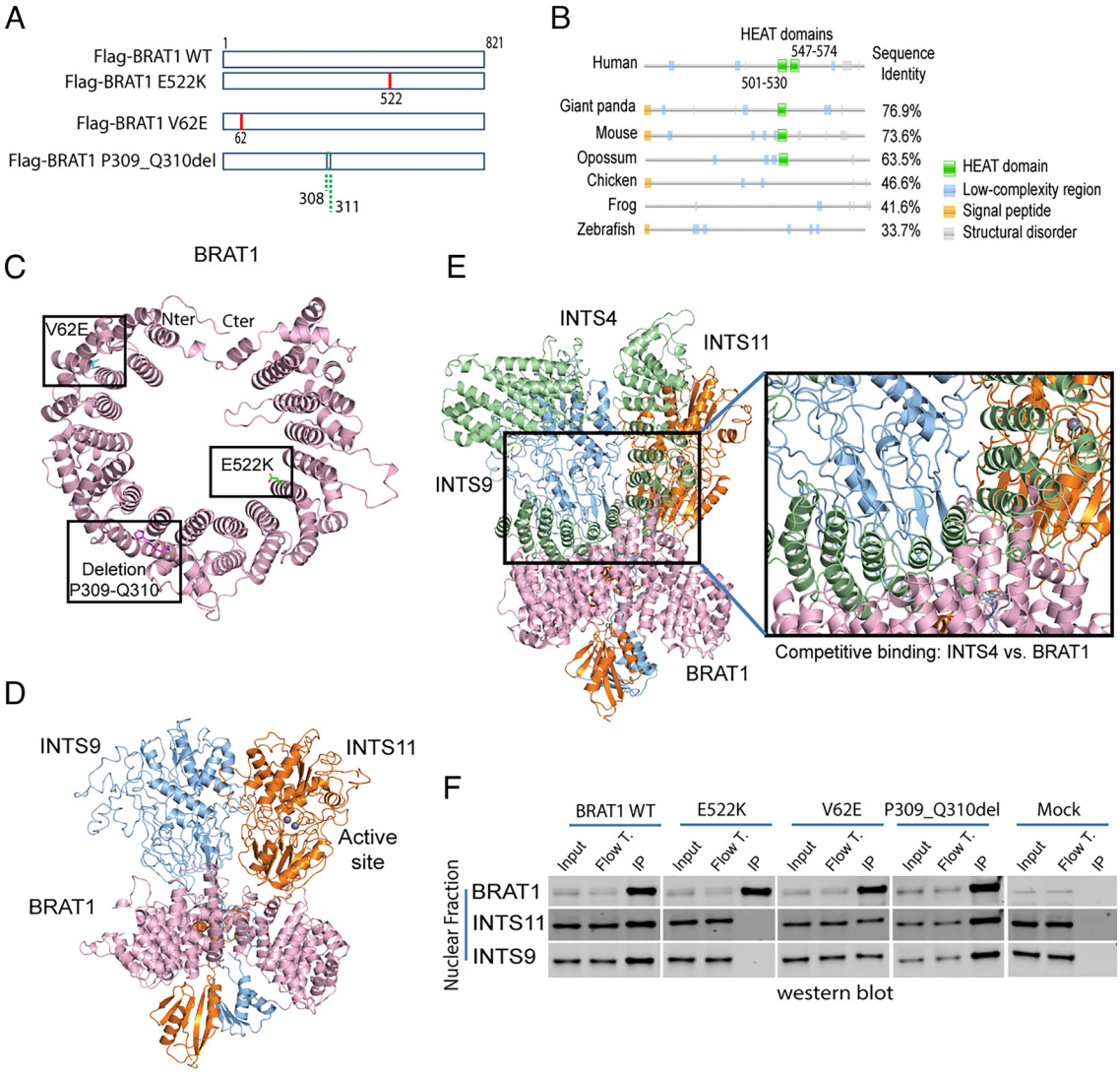

Fig. 5. The pathogenic BRAT1 E522K mutation disrupts BRAT1 interaction with INTS11/INTS9 heterodimer. (*A*) Schematic diagram showing the various constructs used for the investigation of interaction sites between BRAT1 and INTS11/INTS9 heterodimer. In addition to the WT BRAT1 (WT), three mutant constructs were engaged: E522K (c.1564G>A, p.Glu522Lys, red line), V62E (c.185 T>A, p.Val62Glu, red line), and P309_Q310del (c.925_930del p.Pro309_Gln310del, green dash line). (*B*) Protein sequence and domain conservation across representative vertebrate species. Pfam domains are shown as green boxes. Further properties are mapped to the sequence such as signal peptides in orange, low-complexity regions in blue, and structural disorder in gray. Percentage of pairwise sequence identity to the human protein is shown on the right side. Pfam analysis shows that two HEAT domains are located at amino acids 501 to 530 and 547 to 574 ranges in human BRAT1. (*C*) Tridimensional model of the human full-length BRAT1 protein (length = 821 residues). The mutations under analysis were mapped to the structure and highlighted as sticks in different colors (green = E522, cyan = V62, pink = P309-P310del). N-terminal and C-terminal regions are labeled. (*D*) Tridimensional model of the proposed binding mode between BRAT1 (pink), INTS9 (blue), and INTS11 (orange) obtained by molecular docking. The INTS11 active site contains two Zinc ions, shown as purple spheres. (*E*) Overlay of the proposed tridimensional model of BRAT1/INTS9/INTS11 complex to the experimentally resolved cleavage model (INTS4/INTS9/INTS11) (51) showing competitive binding between BRAT1 and INTS4. The detailed zoom on the right side illustrates the multiple clashes between BRAT1 and INTS4, rendering incompatible the interaction of BRAT1 with the full cleavage module and rest of the INTAC subunits. BRAT1, in pink, partially shares the binding interface of INTS4, in green, with the dimer INTS9-INTS11, in blue and orange respectively. (*F*) Site-directed mutagenesis (E522K, V62E, or P309_Q310del) was applied to BRAT1 protein by stable expression of Flag-BRAT1 mutants in HEK293T cells, and then its interaction with INTS11/INTS9 heterodimer was visualized by western blot. HEK293T cells stably expressing Flag-BRAT1 WT isoform and mock were examined as positive and negative controls, respectively.

and INTS4 proteins when overlaying the INTS11/INTS9/BRAT1 complex into the experimental structure of the cleavage module). This result is consistent with our inability to detect BRAT1 in the affinity-purified eluate of Integrator complex isolated through Flag-INTS4 or Flag-INTS6 which are enriched with core-Integrator subunits (*SI Appendix*, Fig. S3). To assess the effect of BRAT1 mutations in the association with INTS11/INTS9 heterodimer, we ectopically expressed the wild type (WT) and three disease-causing Flag-BRAT1 mutations (E522K, V62E, and del_P309-Q310) in HEK293T cells. While the WT and the two amino acids deletion (P309-Q310) of BRAT1 show normal association with INTS11/INTS9, the missense mutations either completely (E522K) or partially (V62E) disrupts the association between BRAT1 and INTS11/INTS9 heterodimer (Fig. 5*F*). These results connect the molecular defect, loss of BRAT1/INTS11/INTS9 interaction, with the phenotypic manifestation of disease phenotype by two disease-causing BRAT1 mutations described in patients with neurodevelopmental disorders (48, 49).

BRAT1 WT and V62E Mutant Rescue the Neuronal Differentiation in *Brat1* Knockout (KO) Mouse Embryonic Stem Cells (mESC). To further dissect the role of BRAT1 in neuronal differentiation and to assess the functional link between INTS11/INTS9, we developed mESC containing a targeted deletion of *Brat1* exon 2 (Fig. 6 *A* and *B*). Mouse ES cells with loss of *Brat1* did not display a growth defect in normal serum media, however they show a growth defect using RHB-A differentiation media (*SI Appendix*, Fig. S4). Next,

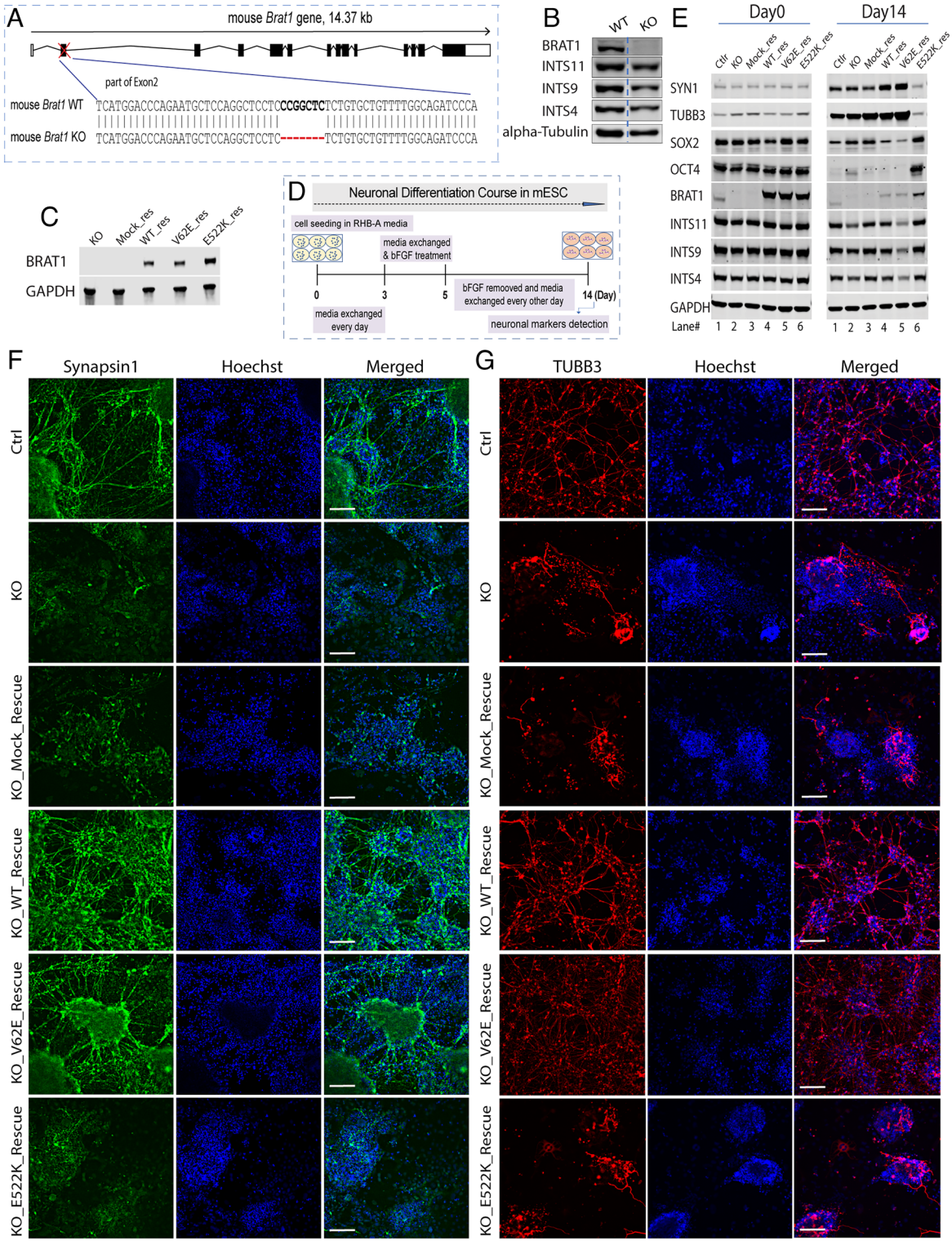

Fig. 6. Neuronal differentiation was lost in BRAT1 E522K mutation unable to interact with INTS11/INTS9 in mESC. (*A*) Schematic diagram of mouse *Brat1* gene. Exons and introns are illustrated by boxes and broken lines, respectively. The sequence of the fragment of WT *Brat1* exon2 which was targeted by CRISPR is shown in black letters. Seven red letters are corresponded to the deleted region in mouse *Brat1* KO which make a frame shift in the sequence. (*B*) Western blot of BRAT1, INTS11, INTS9, and INTS4 in WT and *Brat1* KO mESC. α-Tubulin was used as the control. (*C*) Western blot of BRAT1 in KO, mock-rescue, WT-rescue, V62E-rescue, and E522K-rescue mESCs. GAPDH was used as the control. Res. denotes rescue. (*D*) Diagram of the protocol used for the differentiation of mES cells into neurons. (*E*) Western blot analyses of BRAT1, INTS4, INTS9, and INTS11 in parallel with stemness, and neuronal markers 14 d postdifferentiation of mESCs in *Brat1* KO, *Brat1* WT, and mutants rescue cells compared to control cells. Res. denotes rescue. (*F*) Representative immunofluorescence images of Synapsin1 (green, Synaptic Systems #106 011C3), Hoechst (blue), and merged images in mESCs 14 d post neuronal differentiation. The scale bar for the microscopy images in panels is 100 μm. (*G*) Representative immunofluorescence images of TUBB3 (red, Biolegend #801201), Hoechst (blue), and merged images in mESCs cells 14 d post neuronal differentiation. The scale bar for the microscopy images is 100 μm.

we reconstituted the *Brat1* null ES cells with either WT, V62E, or E522K variants of *Brat1* (Fig. 6*C*). Using an established protocol for neuronal differentiation (Fig. 6*D*) (52, 53), all cell lines were induced to differentiate into a neuronal phenotype. Interestingly, the ES cell expressing V62E form of BRAT1 behaved like WT displaying normal growth rate in RHB-A media and exhibited a neuronal phenotype upon differentiation (Fig. 6 *D*–*G* and *SI Appendix*, Fig. S4). In stark contrast, cells expressing BRAT1 with E522K mutation which is unable to interact with INTS11/INTS9 behaved similar to the null *Brat1* cells displaying growth defect using RHB-A media and failing to differentiate into a neuronal phenotype (Fig. 6 *E*–*G* and *SI Appendix*, Fig. S4). These experiments highlight the importance of BRAT1 in neuronal differentiation and pinpoints the INTS11/INTS9 interaction as an essential feature of BRAT1 function in neuronal differentiation.

Discussion

BRAT1 mutations in humans cause a spectrum of neurodevelopmental disorders often resulting in cerebellar atrophy and rigidity with or without seizures in neonates (9–14). While BRAT1 protein is reported to associate with BRCA1 and ATM proteins (1), our biochemical isolation of BRAT1-containing complexes from human cells identifies INTS11 and INTS9 proteins as the only stably associated components of the BRAT1 complex (Fig. 1). This observation is consistent with a recent report describing BRAT1 interaction with INTS11/INTS9 heterodimer in human cells (54). We find BRAT1 associates with INTS11/INTS9 heterodimer in both HEK293T (Fig. 1) and NT2 (Fig. 2*A*) human cell lines. Our biochemical analyses suggest that BRAT1 and INTS4 are components of distinct INTS11/INTS9-containing complexes. While INTS4 associate with INTS11/INTS9 to form the catalytic module of Integrator complex and allowing for the association of other core Integrator subunits (51), BRAT1 binding to INTS11/INTS9 yields an exclusive trimeric complex. Our modeling of BRAT1 binding to INTS11/INTS9 supports this conclusion revealing a mutually exclusive binding interface between BRAT1 and INTS4 for binding the INTS11/INTS9 heterodimer (Fig. 5*E*). Importantly, the BRAT1 mutation of the key disease-causing residue E522K (48) present at the inner circular structure predicted to bind the C-terminal domain of INTS9/INTS11 completely abrogates BRAT1 interaction with INTS11/INTS9 highlighting the importance of this association in human cells. Additionally, the E522K mutation is unable to rescue the loss of neuronal differentiation in mESC highlighting the importance of BRAT1 association with INTS11/INTS9 proteins.

A previous study suggests that mutation in BRAT1 causes the destabilization of its interaction with INTS11 and INTS9, thereby affecting the 3′-ends processing of UsnRNAs in U2OS cells (54). They also found decreased levels of INTS11 in cell lines derived from patients with BRAT1 mutations. Therefore, using these cell lines, it would be difficult to assess whether BRAT1 directly contributes to RNA splicing defects seen following its depletion, since they may be caused by a secondary consequence of the INTS11 down regulation. Interestingly, in our case, the depletion of BRAT1 in NT2 cells does not affect the levels of INTS11 or INTS9 (Fig. 2*C* and *SI Appendix*, Fig. S1*B*), providing an opportunity to assess the functional consequence of BRAT1 perturbations in the absence of INTS11 loss. Our results suggest a specific effect of BRAT1 on the expression of a set of BRAT1-responsive neuronal genes distinct from the misprocessing of small nuclear RNAs by INTS11 depletion.

Integrator is a multisubunit protein complex implicated in multiple cellular pathways including processing of noncoding and coding transcripts as well as regulation of initiation and elongation of transcription (24, 25, 28, 32, 39, 55). Importantly, mutations in the number of Integrator subunits including INTS11 leads to brain developmental syndromes (40, 41). These findings suggest an overarching role for Integrator as well as BRAT1/INTS11/INTS9 complex in the regulation of neuronal genes. We show that BRAT1 plays an important role in recruiting INTS11 to these genes during their ATRA-mediated differentiation induction. Importantly, we find a dynamic interplay between BRAT1 and neuronal silencer REST. During neuronal differentiation, REST is displaced from critical genes involved in neuronal differentiation. Loss of BRAT1 leads to a persistent residency of REST at neuronal genes resulting in their lack of transcriptional induction during differentiation. Taken together, our study provides a direct link between BRAT1 and INTS11/INTS9 heterodimer in regulation of REST-responsive genes during differentiation of human NT2 cells into a neuronal faith.

Materials and Methods

Methods are described in detail in *SI Appendix*.

Cell Lines. HEK293T cell lines stably expressing Flag-BRAT1, Flag-INTS11, Flag-INTS6, and Flag-INTS4 and mock were established and cultured in DMEM containing puromycin (2.5 μg/mL) and supplemented with 10% FBS. NT2/D1 (NTERA-2 cl.D1) cells, purchased from ATCC (CRL-1973), stably expressing Dox-inducible shControl and sh*BRAT1* were made by tet-pLKO-puro vectors purchased from Addgene (Cat# 21915). Dox (1 μg/mL) was freshly added in the NT2 culture media for BRAT1 depletion.

Affinity Purification of Flag-BRAT1, Flag-INTS11, Flag-INTS6, Flag-INTS4, and Flag-Mock. HEK293T cell lines, stably expressing Flag-BRAT1, Flag-INTS11, Flag-INTS6, and Flag-INTS4 were cultured in DMEM media, and totally, sixty 15 cm^2 dishes of HEK293T cells (for each purification) were harvested for performing the experiments.

For size-exclusion chromatography, nuclear purified Flag-BRAT1 was loaded onto a Superose 6 (increase 10/300 GL) and equilibrated with BC300 buffer. The flow rate was kept at 0.35 mL/min. Then, 0.5 mL fractions were collected and then TCA precipitated.

Western Blotting. Cells were lysed by M-PER mammalian protein extraction reagent (Thermo Scientific, Cat# 78501), protein quantified by BCA protein assay (Thermo Scientific #23250), and 30 μg of the proteins were loaded on 4 to 12% Criterion TGX Stain-Free precast polyacrylamide gels (BIO-RAD, Cat# 5678084) and transferred to nitrocellulose membranes which were subsequently blocked by 5% BSA for 1 h at RT. Membranes were incubated with primary antibodies for overnight at 4 °C followed by three times washing and incubated with fluorescent-conjugated secondary antibodies for 1 h at room temperature.

Mass Spectrometry. Following Flag-INTS11 and Flag-BRAT1 IPs in HEK293T cells, 50 μL of each of the final eluted samples was sent directly for sequencing. Samples were digested in-solution with trypsin and cleaned up using C18 spin column. Tryptic digests were analyzed using a standard 1.5 h LC gradient on the Thermo Q Exactive HF or the Orbi Exactive HF mass spectrometers.

Neuronal Differentiation of NT2 Cells and mESCs. NTERA-2 cl.D1 [NT2/D1] cells were purchased from ATCC and used for neural differentiation by a protocol, as published previously by Peter W. Andrews (44) with some modifications. Differentiation of mESC into neurons was performed using RHB-A media (Takara, #Y40001) (52, 53) in six-well plates.

RNA Extraction, DNase Treatment, cDNA Synthesis, and RT-qPCR. Total RNA was extracted using Trizol reagent according to the manufacturer's protocol (Thermo Fisher Scientific, #15596026). RNA samples were treated by Turbo DNase RNase free Kit (Invitrogen, #AM1907) to remove DNA. Then, 1 μg of total RNA was used for cDNA synthesis by RevertAid First Strand cDNA Synthesis Kit (Thermo Scientific, #K1622) according to the manufacturer's instructions. For RT-qPCR, GAPDH was applied as an internal control.

ChIP-qPCR. All ChIP experiments were performed in two repeats using the appropriate antibodies. The same amount of DNA per sample was used for the ChIP-qPCR experiments.

REST occupancy of BRAT1-responsive genes was investigated using data published on CistromeDB (ID: 46338) and by a dataset for REST target genes retrieved from (https://maayanlab.cloud/Harmonizome/gene_set/REST/ENCODE+Transcription+Factor+Targets). All the REST ChIP-qPCR primers (*SI Appendix*, Table S1) were designed using published ChIP-seq data performed in neuron PFSK-1 cell line by ENCODE ID: GSM803369 and CistromeDB ID: 46338 (56).

RNA Sequencing. First, 500 ng of the total RNA extracted using TRIzol reagent (Thermo Fisher Scientific, #15596026) and treated with DNase RNase free Kit (Cat#AM1907) was used for the library preparation. The quality of total RNA was assessed by running it on 1% agarose gel and visualized by ethidium bromide staining. The RNA samples were depleted from ribosomal RNA and used for the library preparation using the TruSeq Stranded Total RNA Library Prep Kit (Illumina, #20020596) and then sequenced on Illumina NovaSeq to at least 45 million reads (single-end reads, sequence length = 100 bp).

Protein Conservation. Protein domain information was retrieved from Pfam database (version 35) (16). Protein sequence identities were obtained by clustalo (57) using Uniprot IDs of representative vertebrate species: Human = Q6PJG6, Giant panda = D2I4M3, Mouse = Q8C3R1, Opossum = F6TGD0, Chicken = E1BWY6, Frog = F6VIU7, and Zebrafish = Q1RLU1.

3D Modeling. The tridimensional structure of the full-length, human BRAT1 protein (length = 821 residues) was generated by Alphafold model prediction (58, 59) and retrieved from https://alphafold.ebi.ac.uk with the accession code AF-Q6PJG6-F1. We mapped the human mutations under analysis to this structural model. Using HDOCK (60), we docked the BRAT1 model to the INTS9/INTS11 dimer obtained by Cryo-EM (PDB:7cun) (51). We further compared the interaction interfaces of BRAT1 and INTS4 with the INTS9/INTS11 dimer via superimposition of the generated trimeric model into the cleavage module of the experimental structure by structural alignment of the common subunits with the open-source version of pymol (61). The 3D figures were generated with the open-source version of pymol.

Statistical Analysis. Significant differences for ChIP-qPCR, RT-qPCR data, and average number of cell clusters microscopy analysis were determined by unpaired *t* test using GraphPad Prism analysis (*$P < 0.05$, **$P < 0.01$, ***$P < 0.001$).

Data, Materials, and Software Availability. All data needed to evaluate the conclusions in the paper are present in the paper and/or supporting information. All raw and processed RNA-seq data are deposited in GEO under the accession number GSE237396 (62). The mass spectrometry proteomics data have been deposited to the ProteomeXchange Consortium via the PRIDE (63) partner repository with the dataset identifier PXD050622 (64).

ACKNOWLEDGMENTS. We thank the proteomics and metabolomics facility at Wistar Institute for sequencing of the MS samples and Sylvester Comprehensive Cancer Center Onco-Genomics Core Facility for high-throughput sequencing of the RNA-seq samples. We thank current and past members of the Shiekhattar Lab for discussions and preliminary studies on BRAT1/Integrator functions. This work was supported by funding from University of Miami Miller School of Medicine, Sylvester Comprehensive Cancer Center and grants R01GM078455 from the NIH to R.S. Research reported in this publication was supported by the National Cancer Institute of the NIH under Award Number P30CA240139. The content is solely the responsibility of the authors and does not necessarily represent the official views of the NIH.

1. J. A. Aglipay, S. A. Martin, H. Tawara, S. W. Lee, T. Ouchi, ATM activation by ionizing radiation requires BRCA1-associated BAAT1. *J. Biol. Chem.* **281**, 9710–9718 (2006).
2. A. Pourahmadiyan, M. Heidari, H. Shojaaldini Ardakani, S. Noorian, S. Savad, A novel pathogenic variant of BRAT1 gene causes rigidity and multifocal seizure syndrome, lethal neonatal. *Int. J. Neurosci.* **131**, 875–878 (2021).
3. L.-H. Low *et al.*, Ndd4 family interacting protein 1 (Ndfip1) is required for ubiquitination and nuclear trafficking of BRCA1-associated ATM activator 1 (BRAT1) during the DNA damage response. *J. Biol. Chem.* **290**, 7141–7150 (2015).
4. M. Ouchi, T. Ouchi, Regulation of ATM/DNA-PKcs phosphorylation by BRCA1-associated BAAT1. *Genes Cancer* **1**, 1211–1214 (2010).
5. E. Y. So, T. Ouchi, The potential role of BRCA1-associated ATM activator-1 (BRAT1) in regulation of mTOR. *J. Cancer Biol. Res.* **1**, 1001 (2013).
6. E. Y. So, T. Ouchi, BRAT1 deficiency causes increased glucose metabolism and mitochondrial malfunction. *BMC Cancer* **14**, 548 (2014).
7. L. Hu *et al.*, Serum anti-BRAT1 is a common molecular biomarker for gastrointestinal cancers and atherosclerosis. *Front. Oncol.* **12**, 870086–870086 (2022).
8. C. Cui *et al.*, Total synthesis and target identification of the curcusone diterpenes. *J. Am. Chem. Soc.* **143**, 4379–4386 (2021).
9. P. Balasundaram, M. Fijas, S. Nafday, A rare case of lethal neonatal rigidity and multi-focal seizure syndrome. *Cureus* **13**, e13600 (2021).
10. S. Nuovo *et al.*, Clinical variability at the mild end of BRAT1-related spectrum: Evidence from two families with genotype–phenotype discordance. *Human Mutat.* **43**, 67–73 (2022).
11. I. E. Scheffer *et al.*, BRAT 1 encephalopathy: A recessive cause of epilepsy of infancy with migrating focal seizures. *Dev. Med. Child Neurol.* **62**, 1096–1099 (2019).
12. S. A. Mundy, B. L. Krock, R. Mao, J. J. Shen, BRAT1-related disease–identification of a patient without early lethality. *Am. J. Med. Genet. Part A* **170**, 699–702 (2016).
13. S. Srivastava, S. Naidu, Epileptic encephalopathy due to BRAT1 pathogenic variants. *Pediatric Neurol. Briefs* **30**, 45 (2016).
14. S. Srivastava *et al.*, BRAT1 mutations present with a spectrum of clinical severity. *Am. J. Med. Genet. Part A* **170**, 2265–2273 (2016).
15. A. Hernández-Plaza *et al.*, eggNOG 6.0: enabling comparative genomics across 12 535 organisms. *Nucleic Acids Res.* **51**, D389–D394 (2023).
16. J. Mistry *et al.*, Pfam: The protein families database in 2021. *Nucleic Acids Res.* **49**, D412–D419 (2021).
17. I. Sillitoe *et al.*, CATH: Increased structural coverage of functional space. *Nucleic Acids Res.* **49**, D266–D273 (2021).
18. A. M. Duly, F. C. Kao, W. S. Teo, M. Kavallaris, βIII-tubulin gene regulation in health and disease. *Front. Cell Dev. Biol.* **10**, 851542 (2022).
19. J.-I. Satoh, N. Kawana, Y. Yamamoto, ChIP-seq data mining: Remarkable differences in NRSF/REST target genes between human ESC and ESC-derived neurons. *Bioinform. Biol. Insights* **7**, 357–368 (2013).
20. Y.-M. Sun *et al.*, Rest-mediated regulation of extracellular matrix is crucial for neural development. *PLoS One* **3**, e3656 (2008).
21. C. Zuccato *et al.*, Huntingtin interacts with REST/NRSF to modulate the transcription of NRSE-controlled neuronal genes. *Nat. Genet.* **35**, 76–83 (2003).
22. D. Baillat *et al.*, Integrator, a multiprotein mediator of small nuclear RNA processing, associates with the C-terminal repeat of RNA polymerase II. *Cell* **123**, 265–276 (2005).
23. M. M. Pfleiderer, W. P. Galej, Structure of the catalytic core of the Integrator complex. *Mol. Cell* 81, 1246–1259.e1248 (2021).
24. F. Beckedorff *et al.*, The human integrator complex facilitates transcriptional elongation by endonucleolytic cleavage of nascent transcripts. *Cell Rep.* **32**, 107917 (2020).
25. L. F. Dasilva *et al.*, Integrator enforces the fidelity of transcriptional termination at protein-coding genes. *Sci. Adv.* **7**, eabe3393 (2021).
26. T. R. Albrecht *et al.*, Integrator subunit 4 is a 'Symplekin-like'scaffold that associates with INTS9/11 to form the Integrator cleavage module. *Nucleic Acids Res.* **46**, 4241–4255 (2018).
27. Y. Wu, T. R. Albrecht, D. Baillat, E. J. Wagner, L. Tong, Molecular basis for the interaction between Integrator subunits IntS9 and IntS11 and its functional importance. *Proc. Natl. Acad. Sci. U.S.A.* **114**, 4394–4399 (2017).
28. N. Kirstein, H. G. Dos Santos, E. Blumenthal, R. Shiekhattar, The Integrator complex at the crossroad of coding and noncoding RNA. *Curr. Opin. Cell Biol.* **70**, 37–43 (2021).
29. A. Gardini *et al.*, Integrator regulates transcriptional initiation and pause release following activation. *Mol. Cell* **56**, 128–139 (2014).
30. J. R. Skaar *et al.*, The integrator complex controls the termination of transcription at diverse classes of gene targets. *Cell Res.* **25**, 288–305 (2015).
31. B. Stadelmayer *et al.*, Integrator complex regulates NELF-mediated RNA polymerase II pause/release and processivity at coding genes. *Nat. Commun.* **5**, 1–11 (2014).
32. F. Lai, A. Gardini, A. Zhang, R. Shiekhattar, Integrator mediates the biogenesis of enhancer RNAs. *Nature* **525**, 399–403 (2015).
33. J. N. Jodoin *et al.*, The snRNA-processing complex, Integrator, is required for ciliogenesis and dynein recruitment to the nuclear envelope via distinct mechanisms. *Biol. Open* **2**, 1390–1396 (2013).
34. L. D. Kapp, E. W. Abrams, F. L. Marlow, M. C. Mullins, The integrator complex subunit 6 (Ints6) confines the dorsal organizer in vertebrate embryogenesis. *PLoS Genet.* **9**, e1003822 (2013).
35. M. E. Obeidat *et al.*, GSTCD and INTS12 regulation and expression in the human lung. *PloS One* **8**, e74630 (2013).
36. Y. Otani *et al.*, Integrator complex plays an essential role in adipose differentiation. *Biochem. Biophys. Res. Commun.* **434**, 197–202 (2013).
37. M. Xie *et al.*, The host Integrator complex acts in transcription-independent maturation of herpesvirus microRNA 3′ ends. *Genes Dev.* **29**, 1552–1564 (2015).
38. D. Cazalla, M. Xie, J. A. Steitz, A primate herpesvirus uses the integrator complex to generate viral microRNAs. *Mol. Cell* **43**, 982–992 (2011).
39. N. Kirstein *et al.*, The Integrator complex regulates microRNA abundance through RISC loading. *Sci. Adv.* **9**, eadf0597 (2023).
40. R. Oegema *et al.*, Human mutations in integrator complex subunits link transcriptome integrity to brain development. *PLoS Genet.* **13**, e1006809 (2017).
41. L. G. Mascibroda *et al.*, INTS13 mutations causing a developmental ciliopathy disrupt integrator complex assembly. *Nat. Commun.* **13**, 6054 (2022).
42. Z. Dominski, X.-C. Yang, M. Purdy, E. J. Wagner, W. F. Marzluff, A CPSF-73 homologue is required for cell cycle progression but not cell growth and interacts with a protein having features of CPSF-100. *Mol. Cell. Biol.* **25**, 1489–1500 (2005).
43. S. Abolpour Mofrad, K. Kuenzel, O. Friedrich, D. F. Gilbert, Optimizing neuronal differentiation of human pluripotent NT 2 stem cells in monolayer cultures. *Dev. Growth Differ.* **58**, 664–676 (2016).
44. P. W. Andrews, Retinoic acid induces neuronal differentiation of a cloned human embryonal carcinoma cell line in vitro. *Dev. Biol.* **103**, 285–293 (1984).

45. Q. Shao, T. Yang, H. Huang, F. Alarmanazi, G. Liu, Uncoupling of UNC5C with polymerized TUBB3 in microtubules mediates netrin-1 repulsion. *J. Neurosci.* **37**, 5620–5633 (2017).
46. L. Conti *et al.*, Niche-independent symmetrical self-renewal of a mammalian tissue stem cell. *PLoS Biol.* **3**, e283 (2005).
47. A. M. Jurga, M. Paleczna, J. Kadluczka, K. Z. Kuter, Beyond the GFAP-astrocyte protein markers in the brain. *Biomolecules* **11**, 1361 (2021).
48. N. Girard *et al.*, Heterogeneity of chondrosarcomas response to irradiations with X-rays and carbon ions: A comparative study on five cell lines. *J. Bone Oncol.* **22**, 100283 (2020).
49. A. Mahjoub *et al.*, Homozygous pathogenic variant in BRAT1 associated with nonprogressive cerebellar ataxia. *Neurol. Genet.* **5**, e359 (2019).
50. S. Valence *et al.*, Exome sequencing in congenital ataxia identifies two new candidate genes and highlights a pathophysiological link between some congenital ataxias and early infantile epileptic encephalopathies. *Genet. Med.* **21**, 553 (2019).
51. H. Zheng *et al.*, Identification of Integrator-PP2A complex (INTAC), an RNA polymerase II phosphatase. *Science* **370**, eabb5872 (2020).
52. E. Abranches *et al.*, Neural differentiation of embryonic stem cells in vitro: A road map to neurogenesis in the embryo. *PloS One* **4**, e6286 (2009).
53. Q.-L. Ying, M. Stavridis, D. Griffiths, M. Li, A. Smith, Conversion of embryonic stem cells into neuroectodermal precursors in adherent monoculture. *Nat. Biotechnol.* **21**, 183–186 (2003).
54. Z. Cihlarova *et al.*, BRAT1 links Integrator and defective RNA processing with neurodegeneration. *Nat. Commun.* **13**, 1–14 (2022).
55. T.-K. Kim, R. Shiekhattar, Diverse regulatory interactions of long noncoding RNAs. *Curr. Opin. Genet. Dev.* **36**, 73–82 (2016).
56. J. Gertz *et al.*, Distinct properties of cell-type-specific and shared transcription factor binding sites. *Mol. Cell* **52**, 25–36 (2013).
57. F. Sievers *et al.*, Fast, scalable generation of high-quality protein multiple sequence alignments using Clustal Omega. *Mol. Syst. Biol.* **7**, 539 (2011).
58. J. Jumper *et al.*, Highly accurate protein structure prediction with AlphaFold. *Nature* **596**, 583–589 (2021).
59. M. Varadi *et al.*, Alphafold protein structure database: Massively expanding the structural coverage of protein-sequence space with high-accuracy models. *Nucleic Acids Res.* **50**, D439–D444 (2022).
60. Y. Yan, H. Tao, J. He, S.-Y. Huang, The HDOCK server for integrated protein–protein docking. *Nat. Protoc.* **15**, 1829–1852 (2020).
61. W. L. DeLano *et al.*, Pymol: An open-source molecular graphics tool. *CCP4 Newsletter on Protein Crystallography* **40**, 82–92 (2002).
62. S. Dokaneheifard, H. Gomes Dos Santos, M. G. Valencia , H. Arigela , R. Shiekhattar, Data from "BRAT1 associates with INTS11/INTS9 to regulate key neurodevelopmental genes." Gene expression Omnibus (GEO). https://www.ncbi.nlm.nih.gov/geo/query/acc.cgi?acc=GSE237396. Deposited 14 July 2023.
63. Y. Perez-Riverol *et al.*, The PRIDE database resources in 2022: A hub for mass spectrometry-based proteomics evidences. *Nucleic Acids Res.* **50**, D543–D552 (2022).
64. S. Dokaneheifard, R. Shiekhattar, Data from "Neuronal differentiation requires BRAT1 complex to remove REST from chromatin." PRIDE. https://www.ebi.ac.uk/pride/. Deposited 14 March 2024.